Metalloenzymes

DOI: 10.1002/anie.201408693

Iron(III) Located in the Dinuclear Metallo-β-Lactamase IMP-1 by Pseudocontact Shifts**

*Thomas J. Carruthers, Paul D. Carr, Choy-Theng Loh, Colin J. Jackson, and Gottfried Otting**

Abstract: *Heterodinuclear metalloenzymes are an important class of metalloproteins, but determining the location of the different metal ions can be difficult. Herein we present a new NMR spectroscopy method that uses pseudocontact shifts (PCS) to achieve this without assumptions about the coordinating ligands. The approach is illustrated with the dinuclear [FeZn] complex of IMP-1, which is a prototypical metallo-β-lactamase (MβL) that confers resistance to β-lactam antibiotics. Results from single-crystal X-ray diffraction were compromised by degradation during crystallization. With [GaZn]-IMP-1 as diamagnetic reference, the PCSs unambiguously identified the iron binding site in fresh samples of [FeZn]-IMP-1, even though the two metal centers are less than 3.8 Å apart and the iron is high-spin Fe^{3+}, which produces only small PCSs. [FeZn]-MβLs may be important drug targets, as [FeZn]-IMP-1 is enzymatically active and readily produced in the presence of small amounts of Fe^{3+}.*

It is estimated that up to half of all proteins contain metal ion cofactors.[1] While the protein:metal ion stoichiometry can readily be determined by inductively coupled plasma optical emission spectroscopy (ICP-OES) or atomic absorption spectroscopy, the precise location of the metal ions is much more difficult to determine, especially in heterodinuclear active sites. Two metal ions in close proximity are a common motif in metalloenzymes, and zinc and iron are among the most abundant transition-metal ions in metalloenzymes.[2] Established methods, such as extended X-ray absorption fine structure (EXAFS) and electron paramagnetic resonance (EPR), provide information about the metal coordination sphere. To link these data to specific metal binding sites, however, requires independent information about the identity and, often, geometry of the amino acid side chains constituting the metal binding sites. Furthermore, these methods can easily be compromised by 10% of an impurity. X-ray crystallography provides structures at atomic resolution but requires single crystals, which can be challenging to obtain and often require highly specific crystallization conditions. Even then, unambiguous identification of metal-ion positions requires anomalous X-ray scattering experiments, which can be difficult to interpret when a dinuclear site is capable of harboring different metals with different occupancies. Using NMR spectroscopy, we show that pseudocontact shifts (PCS) generated by a paramagnetic ion contain sufficient information to pinpoint the location of the paramagnetic center with an accuracy of a few Ångströms even for a difficult nucleus such as high-spin Fe^{3+}, which generates large paramagnetic relaxation enhancements (PRE) and only small PCSs.[3] The method requires knowledge of the structure of the protein backbone but makes no assumptions about the metal-coordinating environment. Using the 25 kDa MβL IMP-1 as an example, we established that the enzyme readily acquires an [FeZn] heterodinuclear active site, identified the iron as high-spin Fe^{3+}, and located it at one of the two metal sites with clear discrimination between the two sites, which are within 3.8 Å of each other.

IMP-1 is the prototype of over 40 members of the class B1 of MβLs that pose an increasing health risk by generating broadband resistance against β-lactam antibiotics including carbapenems.[4] Located on mobile genetic elements, IMP-1 has been found in hospital strains of different pathogenic bacteria.[5] Available crystal structures of IMP-1 have been modeled with two zinc atoms in the active site.[6,7] The metal ions are essential for the activity and structural integrity of the enzyme.

We found that IMP-1 produced by in vivo overexpression in *Escherichia coli* in the presence of small amounts (25 μM) of $FeCl_3$ in the medium takes up equimolar amounts of iron and zinc as determined by ICP-OES. Even a ten-fold excess of zinc did not entirely suppress the uptake of iron. [FeZn]-IMP-1 was enzymatically active (Table S1).

To establish the binding site of the iron and the distribution of iron and zinc between the two metal sites M_1 and M_2, we initially set out to determine the single-crystal X-ray structure. Notably, however, the single crystals were difficult to grow. The final successful method required several weeks for crystal growth, including an incubation period at 37°C and the inclusion of high concentrations of the metal-ion chelator sodium citrate, leading to decreased metal occupancies. While the overall structure of the protein (Protein Data Bank code 4UAM) was the same as that reported for the wild-type [ZnZn] enzyme,[6] the electron

[*] T. J. Carruthers, Dr. P. D. Carr, Dr. C.-T. Loh, Dr. C. J. Jackson, Prof. G. Otting
Research School of Chemistry
Australian National University
Canberra, ACT 0200 (Australia)
E-mail: gottfried.otting@anu.edu.au

[**] Financial support by the Australian Research Council is gratefully acknowledged. We thank A/Prof. Gerhard Schenk and Dr. Peter Vela for the pET-47b(+) expression vector with the bla_{IMP1} gene, Dr. Ruhu Qi for help with cloning, Ms. Ellen Cliff, Mr. Jia Jiunn Chew, Mr. Jeremy Neeman, and Ms. Katey Dugdale for help with the preparation of selectively ^{15}N-labeled samples, Mrs. Viki Withers for help with ICP-OES measurements, Prof. Thomas Huber and Dr. Thitima Urathamakul for help with mass spectrometry and the staff of the Australian Synchrotron for assistance with the X-ray experiments.

Supporting information for this article is available on the WWW under http://dx.doi.org/10.1002/anie.201408693.

density map also indicated that the crystallization conditions had resulted in partial oxidation of the cysteine residue in the active site to sulfinate, with uncertain impact on the metal-binding preferences of the two sites (Figure 1 A and B). The iron ion was detected at the more buried M_1-site by using anomalous X-ray scattering, collecting data above the Fe-K and Zn-K edges (Figure 1 C–F).[8]

To validate the location of the iron ion in fresh solutions of IMP-1, we performed NMR spectroscopy experiments in the absence of citrate. Compared with [ZnZn]-IMP-1, ^{15}N-HSQC cross-peaks of amides near the active site were absent from the NMR spectra of [FeZn]-IMP-1 and cross-peaks of more remote amides were weakened as a result of PREs (Figure 3 A). The PRE data were insufficiently accurate, however, to discriminate between the two metal sites (Figure S8). Discrimination between the metal sites was achieved by measuring PCSs, using samples of [FeZn]-IMP-1 and its diamagnetic analogue, [GaZn]-IMP-1.

The sequence specific resonance assignment of IMP-1 was performed using uniformly ^{15}N/^{13}C and ^{15}N/^{13}C/^{2}H labeled samples of the [ZnZn] complex, which were prepared in vivo with a large excess of zinc in the medium. The backbone resonance assignments of the diamagnetic complex were readily transferred to the [FeZn] complex, because the chemical shifts differed little between the two forms of the protein. The resonance assignments were submitted to the BioMagResBank with the codes 25063 and 25080. For PCS measurements, the [FeZn] and [GaZn] complexes were prepared by cell-free protein synthesis[10] with selectively ^{15}N-labeled amino acids and controlled supply of metal ions.

Most paramagnetic metal ions are associated with a magnetic susceptibility tensor that is anisotropic and therefore induces PCSs in the protein to which the metal ion is bound. The PCSs arise from through-space interactions between the nuclear spins and the paramagnetic center. They depend on the position of the metal ion and the orientation of the $\Delta\chi$ tensor, which describes the anisotropy of the magnetic susceptibility, relative to the protein. The PCS, $\Delta\delta^{PCS}$, of a nuclear spin is measured in ppm and described by [Eq. (1)][11]

$$\Delta\delta^{PCS} = \frac{1}{12\pi r^3}\left[\Delta\chi_{ax}\left(3\cos^2\theta - 1\right) + \frac{3}{2}\Delta\chi_{rh}\sin^2\theta\cos 2\phi\right] \quad (1)$$

where r, θ, and ϕ are the polar coordinates of the nuclear spin with respect to the principal axes of the $\Delta\chi$ tensor, the magnitude of which is characterized by the axial and rhombic components $\Delta\chi_{ax}$ and $\Delta\chi_{rh}$, respectively. A complete description of the $\Delta\chi$ tensor is given by eight parameters (the x, y, and z coordinates of the metal ion, the α, β, and γ Euler angles describing the orientation of the $\Delta\chi$ tensor relative to the protein coordinates, and $\Delta\chi_{ax}$ and $\Delta\chi_{rh}$). Therefore, measurement of the PCSs of at least eight different spins allows determination of the $\Delta\chi$ tensor, including the location of its origin.[11,12]

PCSs were measured as the amide proton chemical shifts observed in [FeZn]-IMP-1 minus the corresponding chemical shifts in a diamagnetic sample. All the PCSs were very small (less than 0.12 ppm). [ZnZn]-IMP-1 turned out to be inadequate as a diamagnetic reference, which we attribute to small changes in chemical shifts caused by different oxidation states

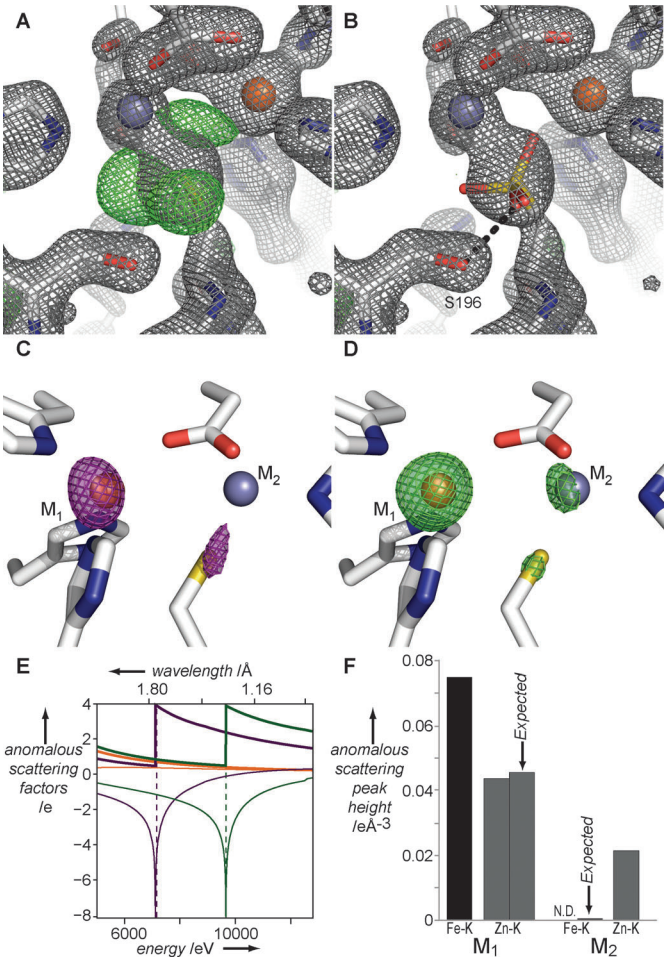

Figure 1. Active site of [FeZn]-IMP-1 determined by X-ray crystallography. The 1.8 Å structure crystallized with a citrate molecule bound to the active site (not shown). The metals in the M_1 (orange sphere) and M_2 (gray sphere) sites are coordinated by three histidine residues, and a histidine, aspartate, and cysteine, respectively. The active-site residues are represented by sticks. The electron densities of the crystal structure indicated about 80% occupancy of the M_1 site with Fe^{3+} and 40% occupancy of the M_2 site with Zn^{2+}. A) $2mF_o-DF_c$ density map (gray mesh at 2.5σ) of the active site. The mF_o-DF_c difference map (green mesh at 4σ) indicated three lobes of positive density around the sulfur of Cys158 indicating partial oxidation. B) Same as (A) except that Cys158 was modeled with two additional conformers of cysteine sulfinic acid, each with a hydrogen bond to Ser196. C) Anomalous scattering map measured above the Fe-K edge, highlighting the location of iron. D) Same as (C), except that the scattering map was measured at the Zn-K edge, highlighting the locations of iron and zinc. The contour levels were chosen to depict the similar level of scattering on the sulfur atom of Cys158. E) Wavelengths used for the anomalous scattering experiments highlighted by dashed lines in a plot of the theoretical anomalous scattering factors, f' (thin lines) and f'' (thick lines), for iron (purple), zinc (green), and sulfur (orange).[9] F) Anomalous scattering peak heights at the M_1 and M_2 sites. The experimental anomalous scattering peak height measured above the Zn-K edge for the M_1 site closely matches expectations if the M_1 site only contains iron.[9] Due to low metal occupancy at the M_2 site, no anomalous scattering signal was detected at the M_2 site above the Fe-K edge, matching expectations if the M_2 site only contains zinc.

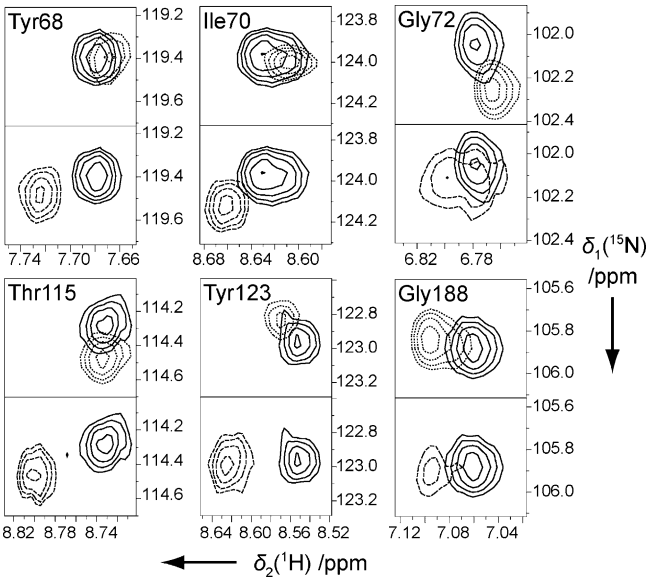

Figure 2. Selected spectral regions from ^{15}N-HSQC spectra of ^{15}N-glycine, ^{15}N-isoleucine, ^{15}N-threonine, or ^{15}N-tyrosine labeled samples of [FeZn], [ZnZn], and [GaZn] complexes of IMP-1. The spectra were recorded of 50 μM solutions of IMP-1 in 20 mM MES buffer, pH 6.5, at 37 °C on a Bruker 800 MHz NMR spectrometer. Top row in each panel: Superimposition of the ^{15}N-HSQC spectra of the [ZnZn] (dotted lines) and the [FeZn] complex (solid lines). Bottom row in each panel: Superimposition of the ^{15}N-HSQC spectra of the [GaZn] (dashed lines) and the [FeZn] complex (solid lines).

of the metal (Fe^{3+} versus Zn^{2+}). The inadequacy of [ZnZn]-IMP-1 as a diamagnetic reference was readily apparent in ^{15}N-HSQC spectra of selectively ^{15}N-labeled samples. For example, the ^{15}N-HSQC cross-peaks were frequently displaced in different directions in the ^{15}N and ^{1}H dimensions (Figure 2; top row in each panel). As the nitrogen and proton of each amide group are very close to each other compared with their distance from the paramagnetic center, similar PCSs are expected for both nuclei.[13] This was indeed the case, when we compared [FeZn] with [GaZn] samples (Figure 2; bottom row in each panel), suggesting that the iron is in the oxidation state 3+, where gallium and iron have very similar ionic radii.

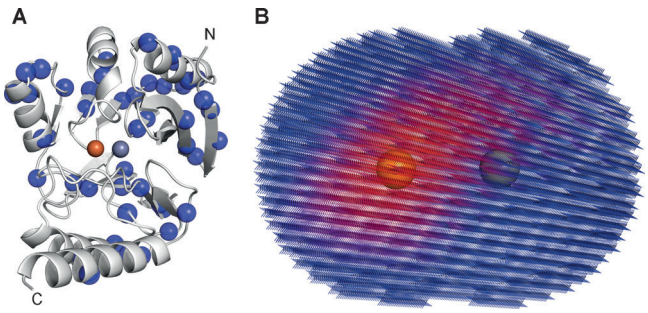

Figure 3. Identification of the paramagnetic center by PCSs. The M_1 and M_2 metal sites in the active site of IMP-1 are depicted as orange and gray spheres, respectively. A) Ribbon drawing of the crystal structure of [FeZn]-IMP-1. Blue spheres highlight the backbone amides of all residues for which a PCS could be measured. Owing to PREs all these amides are at least 11.5 Å from the M_1 site. B) Graphical representation of a grid search around the active site for metal positions with minimal root mean squared deviation (RMSD) between experimental and back-calculated PCS values. The grid points are depicted as crosses that are colored by RMSD values from red (0.023 ppm) to blue (0.028 ppm or greater). The best results cluster around the M_1 site.

A total of 48 PCSs were measured using [GaZn]-IMP-1 as the diamagnetic reference. Using the PCSs as the input to the program PyParaTools,[14] we fitted $\Delta\chi$ tensors to the crystal structure of the [FeZn] complex. A systematic grid search for the best location of the paramagnetic center revealed the M_1 site as the best fitting site (Figure 3).

To assess the oxidation and spin state of the iron, we measured the total paramagnetic susceptibility of [FeZn]-IMP-1 by the experiment by Evans et al.[15] The result indicated a high-spin state with five unpaired electrons, confirming the oxidation state of the iron as Fe^{3+} (Figure S12).

To our knowledge, this is the first time that PCSs have been used for the purpose of accurately locating an Fe^{3+} ion in a protein. High-spin Fe^{3+} is associated with a large but mostly isotropic magnetic susceptibility tensor, resulting in large PREs and small PCSs.[3] Nonetheless, it is much easier to measure accurate PCSs than PREs, which can in part be attributed to the relative insensitivity of PCSs with regard to protein motions and non-specific intermolecular effects. To measure the small PCSs associated with Fe^{3+}, however, a suitable diamagnetic reference proved to be of critical importance. Ga^{3+} is an established structural analogue of Fe^{3+} in dinuclear metalloenzymes.[16] In the case of IMP-1, the [GaZn] complex is, in subtle ways, non-isostructural with the [ZnZn] complex, as chemical shift differences were observed far from the metal site.

This work illustrates the challenge associated with determining the identity, location, and oxidation states of transition metal ions in dinuclear enzymes, as the metal ions may be distributed between the sites with heterogeneous populations (e.g. [FeZn] versus [ZnFe]). The NMR spectroscopy approach presented herein thus adds a uniquely powerful tool to the analysis of metalloenzymes. In particular, NMR spectroscopy would readily detect the presence of any significant heterogeneity in metal composition or location. By using ^{13}C or ^{15}N direct detection, the accuracy with which the paramagnetic center can be located could be enhanced further, provided that the protein is soluble in high concentration.[17]

It is intriguing to speculate on the biological significance of the iron–zinc promiscuity in IMP-1. It is well established that iron stimulates bacterial growth and that bacteria are particularly sensitive to β-lactam antibiotics during cell division. Therefore, maintaining the active enzyme by substituting iron for zinc could provide an advantage under conditions when zinc is scarce but bacterial growth is promoted by iron.

Although mixed-metal active sites with Fe^{3+} are common in dinuclear metallohydrolases,[18] and a glyoxalase II from the wider metallo-β-lactamase superfamily of proteins has been shown to be active with a dinuclear [FeZn] center containing Fe^{3+},[19] all dinuclear MβLs from the subclasses B1–B3 have, to date, been assumed to act predominantly as pure zinc enzymes.[20] The only [FeZn]-MβL investigated to date in some detail has been L1, a subclass B3 MβL, which

was shown to maintain enzymatic activity in the presence of substoichiometric amounts of iron.[21] The ready formation and significant enzymatic activity of the [FeZn] complex of IMP-1 are thus also likely to be features of many other members of the B1 subclass of MβLs, which is the clinically most relevant subclass.[4] The ready uptake of Fe^{3+} poses a new challenge for drug development.

Received: August 31, 2014
Published online: October 15, 2014

Keywords: dinuclear metalloenzymes · IMP-1 · metallo-β-lactamase · NMR spectroscopy · pseudocontact shifts

[1] K. J. Waldron, J. C. Rutherford, D. Ford, N. J. Robinson, *Nature* **2009**, *460*, 823 – 830.
[2] N. Sträter, W. N. Lipscomb, T. Klabunde, B. Krebs, *Angew. Chem. Int. Ed. Engl.* **1996**, *35*, 2024 – 2055; *Angew. Chem.* **1996**, *108*, 2158 – 2191.
[3] I. Bertini, C. Luchinat, *Coord. Chem. Rev.* **1996**, *150*, 1 – 264.
[4] W.-H. Zhao, Z.-Q. Hu, *Crit. Rev. Microbiol.* **2011**, *37*, 214 – 226.
[5] T. R. Walsh, M. A. Toleman, L. Poirel, P. Nordmann, *Clin. Microbiol. Rev.* **2005**, *18*, 306 – 325.
[6] a) N. O. Concha, C. A. Janson, P. Rowling, S. Pearson, C. A. Cheever, B. P. Clarke, C. Lewis, M. Galleni, J.-M. Frère, D. J. Payne, J. H. Bateson, S. S. Abdel-Meguid, *Biochemistry* **2000**, *39*, 4288 – 4298; b) J. H. Toney, G. G. Hammond, P. M. D. Fitzgerald, N. P. Sharma, J. M. Balkovec, G. P. Rouen, S. H. Olson, M. L. Hammond, M. L. Greenlee, Y.-D. Gao, *J. Biol. Chem.* **2001**, *276*, 31913 – 31918; c) H. Kurosaki, Y. Yamaguchi, T. Higashi, K. Soga, S. Matsueda, H. Yumoto, S. Misumi, Y. Yamagata, Y. Arakawa, M. Goto, *Angew. Chem. Int. Ed.* **2005**, *44*, 3861 – 3864; *Angew. Chem.* **2005**, *117*, 3929 – 3932; d) H. Kurosaki, Y. Yamaguchi, H. Yasuzawa, W. Jin, Y. Yamagata, Y. Arakawa, *ChemMedChem* **2006**, *1*, 969 – 972.
[7] a) Y. Yamaguchi, T. Kuroki, H. Yasuzawa, T. Higashi, W. Jin, A. Kawanami, Y. Yamagata, Y. Arakawa, H. Kurosaki, *ChemBioChem* **2011**, *12*, 1979 – 1983; b) L. B. Horton, S. Shanker, R. Mikulski, N. G. Brown, K. J. Phillips, E. Lykissa, B. V. Venkataram Prasad, T. Palzkill, *Antimicrob. Agents Chemother.* **2012**, *56*, 5667 – 5677.
[8] C. J. Jackson, P. D. Carr, H.-K. Kim, J.-W. Liu, P. Herrald, N. Mitić, G. Schenk, C. A. Smith, D. L. Ollis, *Biochem. J.* **2006**, *397*, 501 – 508.
[9] E. A. Merritt, http://skuld.bmsc.washington.edu/scatter.
[10] K. Ozawa, M. J. Headlam, P. M. Schaeffer, B. R. Henderson, N. E. Dixon, G. Otting, *Eur. J. Biochem.* **2004**, *271*, 4084 – 4093.
[11] I. Bertini, C. Luchinat, G. Parigi, *Prog. Nucl. Magn. Reson. Spectrosc.* **2002**, *40*, 249 – 273.
[12] C. Schmitz, M. J. Stanton-Cook, X.-C. Su, G. Otting, T. Huber, *J. Biomol. NMR* **2008**, *41*, 179 – 189.
[13] M. John, G. Otting, *ChemPhysChem* **2007**, *8*, 2309 – 2313.
[14] M. Stanton-Cook, X.-C. Su, G. Otting, T. Huber, http://comp-bio.anu.edu.au/mscook/PPT.
[15] a) D. F. Evans, *J. Chem. Soc.* **1959**, 2003 – 2005; b) S. K. Sur, *J. Magn. Reson.* **1989**, *82*, 169 – 173.
[16] a) M. Merkx, B. A. Averill, *Biochemistry* **1998**, *37*, 8490 – 8497; b) S. J. Smith, A. Casellato, K. S. Hadler, N. Mitić, M. J. Riley, A. J. Bortoluzzi, B. Szpoganicz, G. Schenk, A. Neves, L. R. Gahan, *J. Biol. Inorg. Chem.* **2007**, *12*, 1207 – 1220.
[17] C. Caillet-Saguy, M. Delepierre, A. Lecroisey, I. Bertini, M. Piccioli, P. Turano, *J. Am. Chem. Soc.* **2006**, *128*, 150 – 158.
[18] N. Mitić, S. J. Smith, A. Neves, L. W. Guddat, L. R. Gahan, G. Schenk, *Chem. Rev.* **2006**, *106*, 3338 – 3363.
[19] O. Schilling, N. Wenzel, M. Naylor, A. Vogel, M. Crowder, C. Makaroff, W. Meyer-Klaucke, *Biochemistry* **2003**, *42*, 11777 – 11786.
[20] C. Bebrone, *Biochem. Pharmacol.* **2007**, *74*, 1686 – 1701.
[21] a) Z. Hu, T. S. Gunasekera, L. Spadofora, B. Bennett, M. W. Crowder, *Biochemistry* **2008**, *47*, 7947 – 7953; b) Z. Hu, G. Periyannan, B. Bennett, M. W. Crowder, *J. Am. Chem. Soc.* **2008**, *130*, 14207 – 14216.

